

We are IntechOpen, the world's leading publisher of Open Access books Built by scientists, for scientists

6,900

Open access books available

186,000

International authors and editors

200M

Downloads

Our authors are among the

154

Countries delivered to

TOP 1%

most cited scientists

12.2%

Contributors from top 500 universities



WEB OF SCIENCE™

Selection of our books indexed in the Book Citation Index
in Web of Science™ Core Collection (BKCI)

Interested in publishing with us?
Contact book.department@intechopen.com

Numbers displayed above are based on latest data collected.
For more information visit www.intechopen.com



Comparison of Different Techniques for Measurement of Soot and Particulate Matter Emissions from Diesel Engine

Richard Viskup

Abstract

The research presented here is the comparison studies between different commercially available techniques for measurement of soot and particulate matter (PM) emissions from passenger car diesel engine. The compared devices are filter paper-type smoke meter, photoacoustic spectrometer, opacimeter, differential mobility spectrometer and laser-induced incandescence. The focus is to study static and dynamic transient exhaust emissions from the location position closer to the actual combustion event—downstream of the turbine, position characterised by the higher temperature and higher pressure of the emission gas—than the standard measurement position, in the tailpipe of the exhaust manifold. The main task is to compare an accuracy and sensitivity of individual devices at static and dynamic soot and PM emissions.

Keywords: soot emission, particulate matter, diesel engine, smoke meter, photoacoustic spectroscopy, opacimeter, differential mobility spectrometer, laser-induced incandescence

1. Introduction

The combustion engine-driven vehicles are one of the main consumers of petroleum natural resources and are mainly responsible for air pollution in the heavily traffic regions, in the cities and in large metropolitan areas [1, 2]. To minimise the pollutant emission from vehicles, an effective combustion control and monitoring plays a very important role [3]. Measurements of diesel emissions are usually performed by using various measurement techniques [4]. The limits for exhaust emission of newly produced vehicles are regulated in the European Union (EU) by European emission standards and are defined in a series of European Union directives. These regulations are usually amended every half of the decade and are published in a form of standards like first Euro 1 norm set in year 1992 to current Euro 6 valid from year 2014. In the case of passenger cars, the emission standards are defined for particulate matter (PM), total hydrocarbon, non-methane hydrocarbon (NMHC), carbon monoxide and nitrogen oxide emissions. The basic idea of these norms is to contribute to the reduction of emissions by newly produced vehicles. However, with the strict limits given by the European regulation on pollutant emission, measurement of low-level emission concentrations from the engine is very

challenging. This is mainly due to measurements of such as low concentrations and/or very short time duration peak emissions. Thus, the sensitivity of method and applied measurement techniques represent an important issue [5, 6]. Another important factor for minimising overall emissions is a high temporal resolution of the measurement device, mainly during the measurement of fast transient emission peaks. These are the emissions produced due to the rapid acceleration or deceleration phase of the vehicle. Nowadays there exist many different commercially available techniques for PM and soot concentration emission measurement, based on gravimetric analyses [7], paper filter-type smoke meter [8], measurement of continuous opacity [9, 10], differential mobility spectrometers [11–13], measurement of photoacoustic spectroscopy [14–16] and measurement of laser-induced incandescence (LII) [17–20].

The main differences between these techniques are in methodology and in measurement principle. Another issue is the sensitivity of the measurement itself, sampling time and dynamics response to fast emission detection. Additional criterion is the position—location of sensor during the measurement of emissions from engine. The optimal position of the sensor with respect to the measurement of the fast dynamic response would be as close as possible to the emission source, directly into the combustion chamber of the engine. The second alternative would be upstream of the turbine and the third possibility is downstream of the turbine in the exhaust manifold. The first position—directly into the combustion chamber—is due to the geometrical restrictions that are difficult to measure, and therefore the nearest possible location is in the exhaust manifold. However, due to high instantaneous pressure and temperatures of soot in this part, the measurements are usually performed far from exhaust manifold or directly in the tailpipe. The placement of the sensors into the tailpipe is introducing additional delay in measured emission signal and can negatively influence measured results. A next drawback of tailpipe position is the change in gas emission dynamics due to measurement in lower-pressure zone; however, high-pressure information can be very helpful in order to better characterise, control and minimise emissions during combustion process.

Up to now, the systematic studies dedicated to the differences in sensitivity and accuracy of transient PM emission by comparing available commercial devices were made by Viskup et al. in [21, 22]. The accuracy and reliability of measured emission data are very important information to eliminate toxic emissions from vehicle engines and to meet the future EU directives.

In this chapter, the comparison between different techniques for measurement of soot and particulate matter static as well as dynamic transient emissions is shown. The analysis presents differences in measured emission by individual techniques from a position closer to the actual combustion event, downstream of the turbine in the exhaust manifold. Measurement at this position is influenced by higher temperatures and higher pressures of emission gases than standard tailpipe position. However, this will influence the possibility of using a particular device as well as techniques for such a non-standard measurement location. High concern is given to comparing the device's sensitivity and dynamics at static as well as fast transient emission peaks, because these produce a main fraction of total emissions during the standardised test cycles from passenger car diesel engines [23]. The obtained results will allow better understanding of PM emissions, support dynamic emission modelling for control design and contribute to the development of virtual emission sensors [24, 25].

2. Instrumentation

Because this chapter is dedicated to the comparison between different commercial available measurement devices for the soot and particulate matter emission measurements, the basic measurement principle of each method is briefly discussed.

2.1 Basic principle of differential mobility spectrometer

The basic principle of differential mobility spectrometer (DMS) is in charging of PM particles formed during the combustion and classifying them on the basis of its mobility. Particles of PM, which enter into differential mobility spectrometer, are charged by means of corona discharge. Each particle is charged proportionally to its surface area. Charged particles are then introduced into a strong radial electrical field inside a classifier column. Positively charged particles are further drifting through a sheath flow in the direction of the numerous segmented collection electrodes. Particles are then attached to different distances of the segmented electrode rings down the classifier column, according to their drag charge ratio. The current produced by particles on every sensitive electrometer is used to determine particle size and number of concentration. Basic schema of DMS is shown in **Figure 1**.

2.2 Basic principle of laser-induced incandescence

The laser-induced incandescence technique uses the laser radiation with short pulse duration and high power to irradiate particles formed during the combustion event. This process induces incandescence light emitted by the particulates, which is consecutively detected by fast photodiode, photomultiplier tube (PMT) or fast avalanche photodiode detector (APD) with nanosecond (ns) response time. The excitation of the soot particles by laser-induced incandescence is typically performed with pulsed laser radiation, e.g. Nd:YAG with pulse duration of 10 ns at fundamental laser wavelength 1024 nm with laser fluence $\sim 0.4 \text{ J/cm}^2$ or frequency-doubled 532 nm at $\sim 0.2 \text{ J/cm}^2$ [26]. The basic optical arrangement of LII setup is shown in **Figure 2**.

The LII scheme works as follows. The pulsed laser beam with Gaussian profile is converted into a homogeneous vertical sheet by using a combination of cylindrical and spherical lenses to achieve uniform intensity over spatial profile. Beam is then expanded and directed into the burner. Laser power meter and beam profiler monitors the emerging laser beam from the burner cell. Signal from LII emission is collected perpendicularly by the collecting lens and directed through attenuator into the beam splitter. Split signal is further filtered with interference filters and imaged into fast detector. The LII signal is sampled with nanosecond intervals with fast digital oscilloscope and further processed by the computer.

2.3 Basic principle of opacimeter

The basic principle of the opacimeter is measurement of attenuation of emitting light from the light source, which is transmitted through soot media and

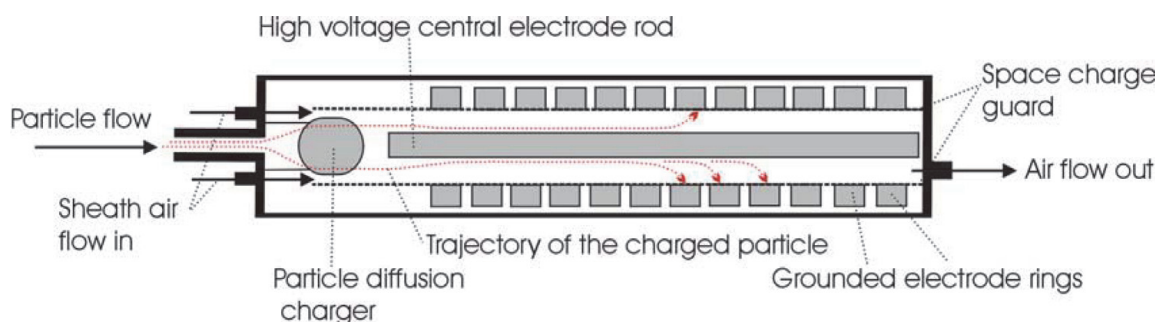


Figure 1.
Schema of differential mobility spectrometer.

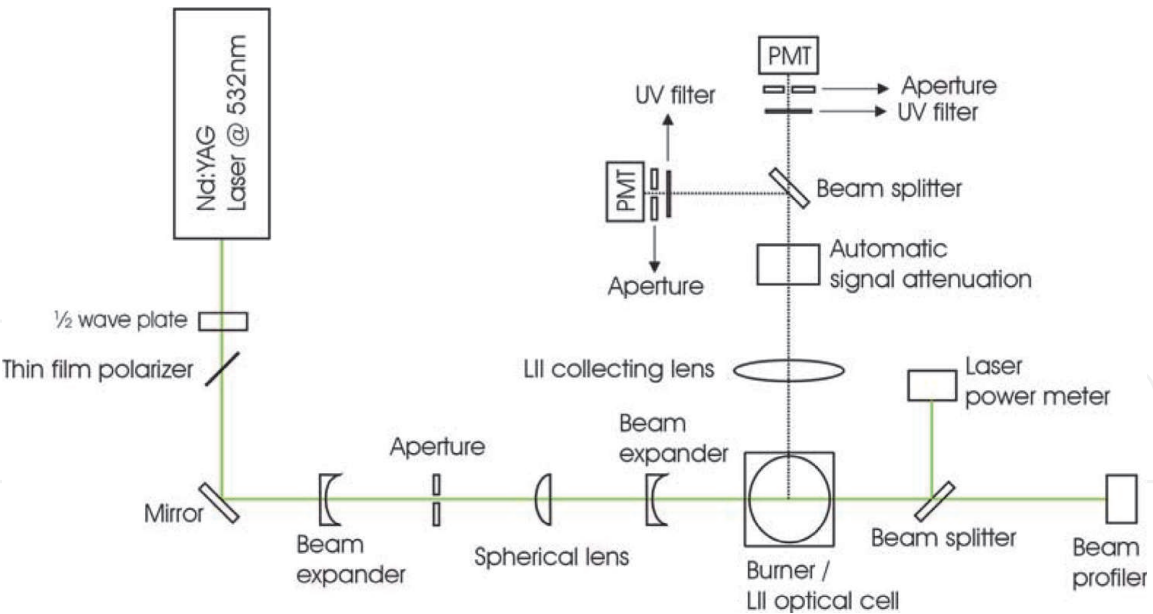


Figure 2.
Optical arrangement of laser-induced incandescence.

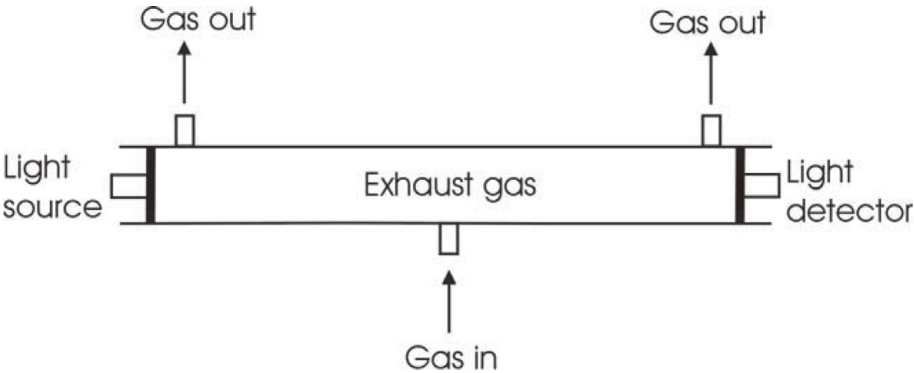


Figure 3.
Schematic arrangement of opacimeter.

consequently absorbed. A light transmitting-type opacimeter measures a soot concentration based on absorbed and scattered light. The measured density value is then the superposition of the black smoke (soot) due to high temperature fuel combustion, blue smoke hydrocarbon vapour and white smoke water vapour. The concentration of the soot is calculated from light attenuation using the Beer-Lambert law of light absorption. The measured results are then expressed as opacity (%) or in absorption coefficient in (m^{-1}). Basic schematic arrangement of the opacimeter is shown in **Figure 3**.

2.4 Measurement of soot concentration from the opacity

Because the opacimeter measures the opacity in %, it is necessary to recalculate the opacity values into soot concentrations. For this reason, the steady-state measurement outputs of the opacimeter and the smoke meter empirical correlation function can be used as:

$$\text{Opacity} = 1.67.FSN^2 + 1.56.FSN + 0.619 \quad (1)$$

which has been derived in [27], to obtain the filter smoke number (FSN) from opacity measurements. The soot concentration can be calculated from the empirical correlation equation [28].

$$\text{Soot (mg/m}^3\text{)} = \frac{1}{0.405} 4.95 \cdot \text{FSN} \cdot e^{(0.38 \cdot \text{FSN})} \tag{2}$$

By this empirical correlation method, it is possible to obtain the soot concentration values in (mg/m³).

2.5 Basic principle of paper filter-type smoke meter

The basic principle of the smoke meter is in measurement of exhaust gas emissions sucked through a filter paper. The blackening of filter paper is measured with reflectometer and indicates the soot content in the exhaust gas. Smoke collected by the filter and the blackening of this filter depend primary on soot concentration and the effective filter length—exhaust gas volume related to the filter area. The measuring principle of the smoke meter is shown in **Figure 4**.

Rolled filter paper is fed through exhaust gas chamber where the soot particles are adsorbed at the surface. Afterwards the filter paper is further moved in the direction of the measurement section. Here the blackening of filter paper is measured with reflectometer and further directed out from this chamber. Used filter paper is rolled on the spool.

2.6 Basic principle of photoacoustic spectroscopy

The basic mechanism of photoacoustic spectroscopy is in measurement of acoustic response after absorption of modulated laser radiation by the PM. The laser radiation is absorbed by the PM and leads to heating and consequently to thermal expansion of the particles accompanied by acoustic waves in surrounding gas of the photoacoustic cell. Local expansion is modulated with the frequency of the light source. Generated sound waves resulting from the modulation of the light are

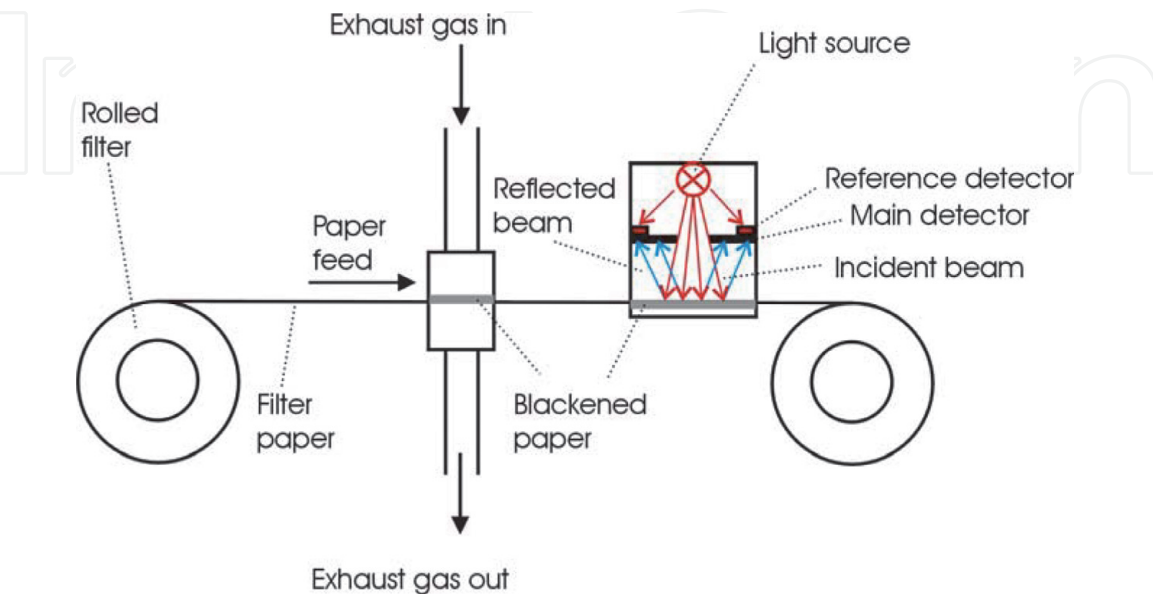


Figure 4.
Measuring principle of paper filter-type smoke meter.

proportional to the absorbed laser energy. Sound waves are recorded by means of sensitive microphone built in the resonator. Intensity of the acoustic waves is proportional to the photoacoustic signal. Acoustic resonator acts as a longitudinal resonator for the amplification of the photoacoustic signal. Speaker is used to determine the exact resonance frequency and for controlling of microphone. Schematic arrangement of photoacoustic spectrometer is shown in **Figure 5**.

3. Experimental

Measurements of particulate matter emissions and soot were performed on Euro 5 standard passenger car diesel engine and on dynamic engine test bench system by applying the following measurement techniques:

1. Photoacoustic spectroscopy—AVL Micro Soot Sensor 483
2. Differential mobility spectrometer—Cambustion DMS500
3. Opacimeter—AVL Opacimeter 439
4. Laser-induced incandescence—Artium Technologies Inc. LII 200
5. Filter-type smoke meter—AVL Smoke meter 415 S

Comparison of basic technical parameters—sensitivity, response, rise and sampling time, upper temperature and upper pressure limits of devices—is shown in **Table 1**.

All instruments were used simultaneously during measurements. Devices were placed downstream of the turbine location in the exhaust manifold part, as is shown in **Figure 6**.

It has to be mentioned that measurement location downstream of the turbine—position before the oxidising catalyst—is characterised by the higher temperature and higher pressure of the emission gases. Therefore, this position can influence the measured results from devices which are more sensitive for higher temperatures or pressures.

The test bench system has been controlled via AVL Puma Open test system automation. The Micro Soot Sensor and opacimeter were connected via dSPACE, DS 1006 Processor and DS2202 HIL I/O Board. Sampling time was set to 4 ms. Data acquisition of laser-induced incandescence device was controlled via the Artium computer, due to the lack of output connection into dSpace, with a sampling time of

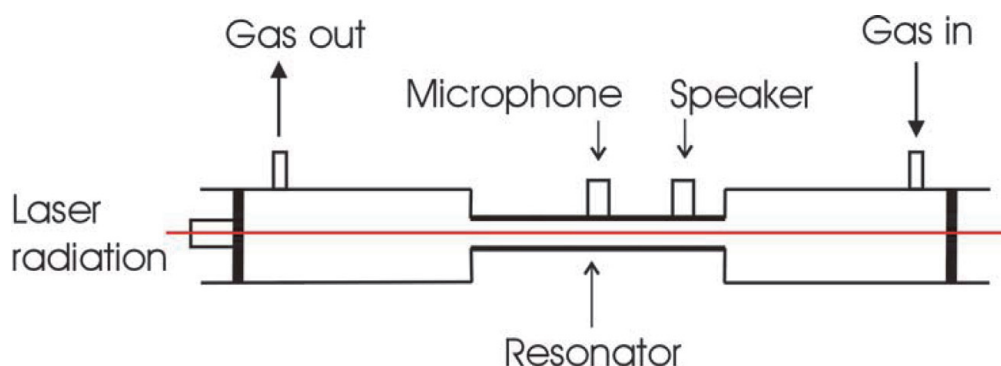


Figure 5.
Schematic arrangement of the photoacoustic spectrometer.

Method / Device	Sensitivity	Time	Upper temperature limit	Upper pressure limit
Laser induced incandescence Artium Technologies LII-200	$\sim 2 \mu\text{g}/\text{m}^3 + \sim 20\text{g}/\text{m}^3$	100ms response time	300°C	5000 mbar
Photo-acoustic spectroscopy Micro soot sensor AVL 483	$\sim 5 \mu\text{g}/\text{m}^3 + \sim 50\text{mg}/\text{m}^3$	1000ms rise time	1000°C	2000 mbar
Opacimeter AVL 439 Opacimeter with high pressure option	0.1% opacity or 0.0025m^{-1} absorption	100ms rise time	600°C 800°C	400 mbar 3000 mbar
Filter type smoke meter AVL - 415S	$\sim 20 \mu\text{g}/\text{m}^3 + \sim 10\text{mg}/\text{m}^3$	1s–100s sampling time	600°C	400 mbar
Differential mobility spectrometer Cambustion model DMS 500	from $\sim 2 \mu\text{g}/\text{m}^3$	200ms response time	150°C	2000 mbar

Table 1.
Specifications of different commercial devices for soot measurement. Upper temperature and pressure limits are for location of sensors in exhaust manifold position.

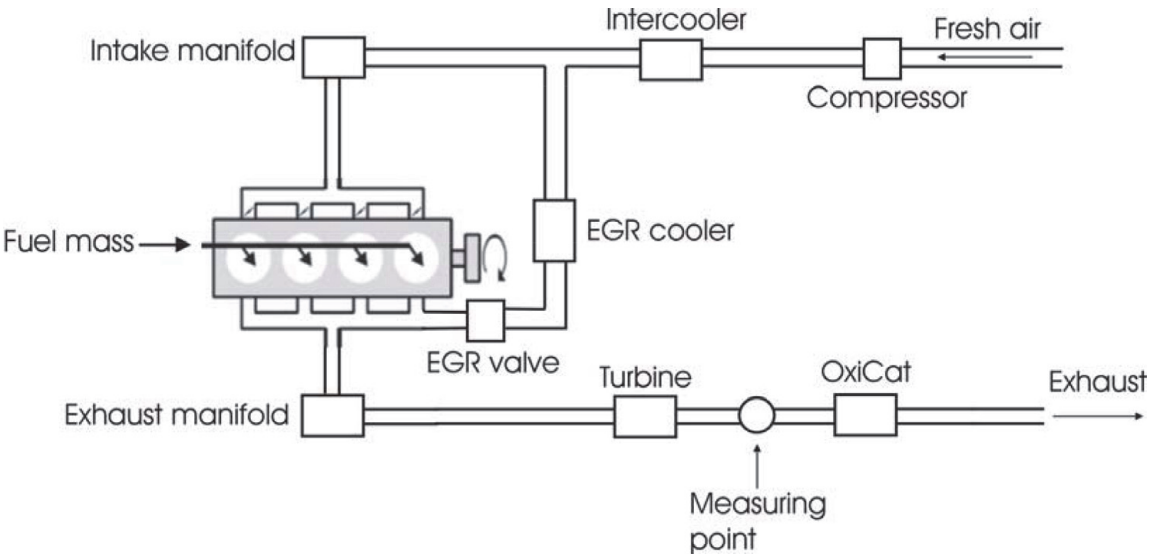


Figure 6.
The schema of the experimental setup and position location of devices during the soot emission measurement. EGR is the engine exhaust gas recirculation, and OxiCat is the oxidising catalyst.

50 ms. A signal from fast differential mobility spectrometer was recorded via both dSpace board and also Cambustion computer with sampling time of 100 ms.

The experiments performed were mainly focused on measurement of soot and particulate matter emissions from diesel engine during static and dynamic transient cycle with special concern to compare the sensitivity and dynamics response of individual devices. The following measurements were performed:

a. Static measurements

To compare a sensitivity of applied instruments at specified input parameters, measurements of relatively long constant and continuous soot emissions (100 second) in the form of rising and falling steps were performed. This time was sufficiently enough for devices to respond on changes in soot level of injected fuel volume in a well-defined time. Injection of fuel volume gradually increases in the form of steps.

b. Pulsed fuel injection

Measurement of soot emission response related to fuel injection in the form of short pulses, with injected well-defined fuel volume (1 or 2 mg/cycle) during a

relatively short time (1 second, 500 or 250 ms), to observe the sensitivity of individual devices, was also performed.

c. Dynamic transient measurements

To compare instruments at transient emission measurement conditions, a New European Driving Cycle (NEDC) has been chosen to analyse a sensitivity and response time of individual devices.

4. Results and discussion

4.1 Static measurements: measurement of constant soot emissions

In the case to study the static emissions from diesel engine, 100-second constant and continuous soot emissions, in the form of rising and falling steps, were measured. With the Puma control system, the defined volume of diesel fuel was injected into the engine. This injection function (fuel set) is shown in the first graph of **Figure 7**. The real injected volume has been also measured, and its profile is shown in the figure as “fuel actual.” Both values have the same unit mg/cycle. In the second graph of **Figure 7**, the engine speed in rotation per minute unit (rpm) is shown. In the third graph, filtered data of soot concentration in mg/m^3 measured by photoacoustic spectroscopy, differential mobility spectrometer, opacimeter, laser-induced incandescence and filter-type smoke meter are shown.

Data recorded by filter-type smoke meter are constant over the individual steps of measurements. This is due to the fact that smoke meter is constructed to measure soot level during longer accumulation time. This is also the reason why the smoke meter has not been used for dynamic transient measurements but rather for static map test.

For very low soot emissions—below $\sim 1 \text{ mg}/\text{m}^3$, in the case of opacimeter—the calculated soot values from the opacity are not so accurate, as the opacimeter

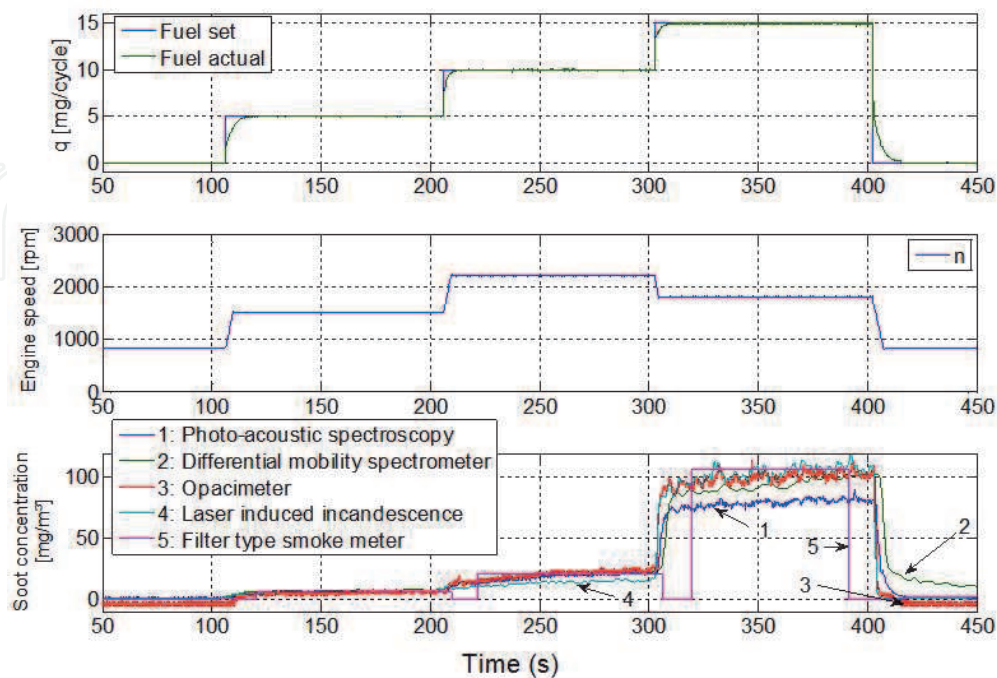


Figure 7.

Figure shows static measurement of soot emissions. Input parameters are injected fuel set, fuel actual and engine speed. Soot concentration in mg/m^3 was measured by photoacoustic spectroscopy, differential mobility spectrometer, opacimeter, laser-induced incandescence and filter-type smoke meter.

measures also the opacity for the zero soot signal. This happens because the exhaust vapour and gases influence the opacity signal too, as the light rays from the opacimeter source scatters on this matter into the detector. Additional error is for small values of opacity, due to recalculation of opacity to soot concentration values using formulas (1) and (2).

For the moderate soot emissions, approximately 5 mg/m^3 , all instruments show more or less the same soot level. In the case of middle soot emission concentrations, $\sim 20 \text{ mg/m}^3$, the values measured by laser-induced incandescence are lower than the values measured by the other methods. For high soot emission concentrations, $\sim 100 \text{ mg/m}^3$, only photoacoustic spectroscopy shows lower level of the soot. At high level of soot emissions, one can easily observe oscillations in measured soot signal, captured by fast dynamic measurement devices.

4.2 Fuel pulse response measurements at constant engine speed

To further characterise a performance of individual methods, mainly the sensitivity to fuel volume and resulting emissions, the soot concentration from well-defined injected fuel volume was investigated. To this end, at the certain level (10.7 mg/cycle) of engine load, a defined volume of additional fuel—1 or 2 mg/cycle—during a short time of 1 second, 500 or 250 ms, was injected in the form of short pulses into the engine, while all devices measured the soot emission response. The results are shown in **Figure 8**.

The fuel injections were performed extra to constant engine load, whereas the engine speed was kept constant at 1800 rpm. From this measurement, one can clearly observe emission peaks related to each fuel injection. A difference in measured peaks is that the certain technique resolved individual fuel injection and consequent soot emission with better resolution. Indeed, some devices show broader pulse width and different shape profile. The peaks measured by

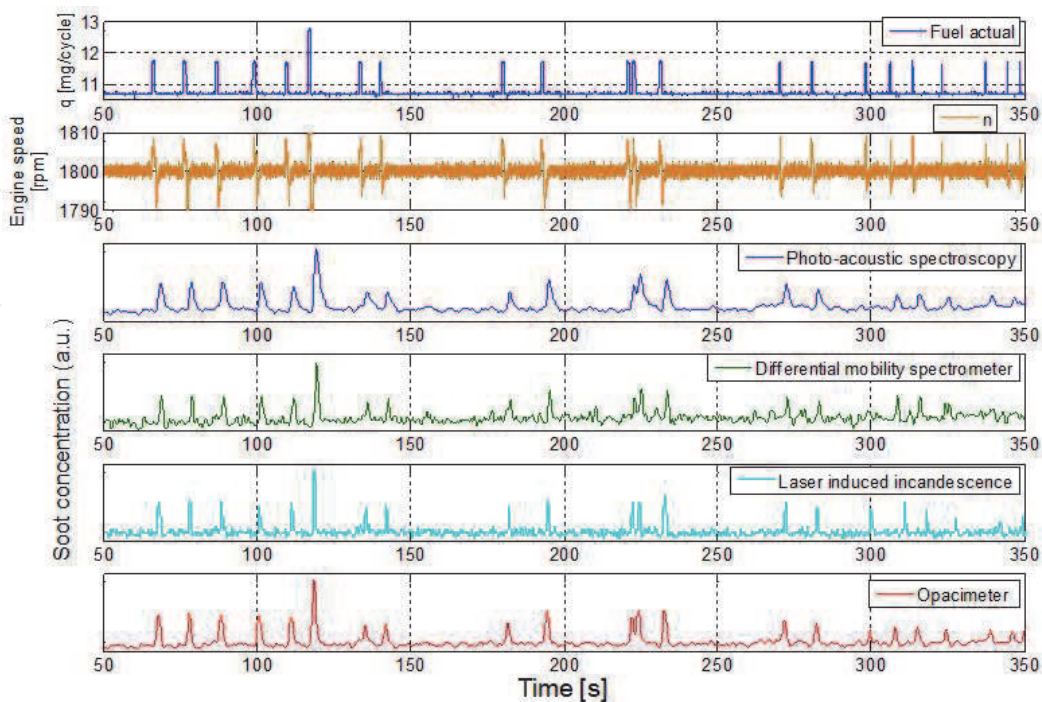


Figure 8. Figure shows the injected fuel, engine speed and filtered data of soot concentration measured by photoacoustic spectroscopy, differential mobility spectrometer, opacimeter and laser-induced incandescence within 1000, 500 and 250 ms injection time at 10.7 mg/cycle fuel load.

the photoacoustic spectroscopy are generally broader than peaks measured by the other methods.

A detailed picture of three injected peaks (two consequent) and measured soot emission response is shown in **Figure 9**. From filtered data in **Figure 9**, one can observe very fast response measured by laser-induced incandescence where two sequential peaks separated by 1 second are well resolved (time scale between 220 and 230 seconds). In the case of differential mobility spectrometer, photoacoustic spectroscopy and opacimeter, the peaks are less pronounced.

4.3 Comparison of dynamics from injected pulse emission peak

The comparison of dynamics was made from measurement of short emission pulses. The main concern was to compare fast dynamics response of individual devices during a well-defined injected fuel volume in the form of short pulses. Due to that reason, one single pulse from this injection which has been further analysed in detail is selected. In **Figure 10** the fuel peak profile with 2 mg/cycle injected during 1 second, corresponding engine speed profile and raw data of soot concentration measured at 10.7 mg/cycle load are shown. The shape of the engine speed curve is increasing due to injected fuel volume up to 1808 rpm and consecutively decelerating due to dynamometer braking force. Dynamometer further compensates an engine speed to 1800 rpm. The event from the fuel injection with rectangular profile function lasts approximately 1000 ms, while the engine speed response (with reversed profile) to this injection lasts approximately 2000 ms. After that time (2000 ms), the engine speed settles to a constant value of 1800 rpm. Consequently, measured response to soot emission is broadening of peak function in direction to later times (to right side). The peak response measured by laser-induced incandescence lasts 1500 ms; in the case of differential mobility spectrometer, it lasts 1700 ms; for opacimeter it lasts 2900 ms; and in the case of photoacoustic spectroscopy, it lasts 4400 ms. From

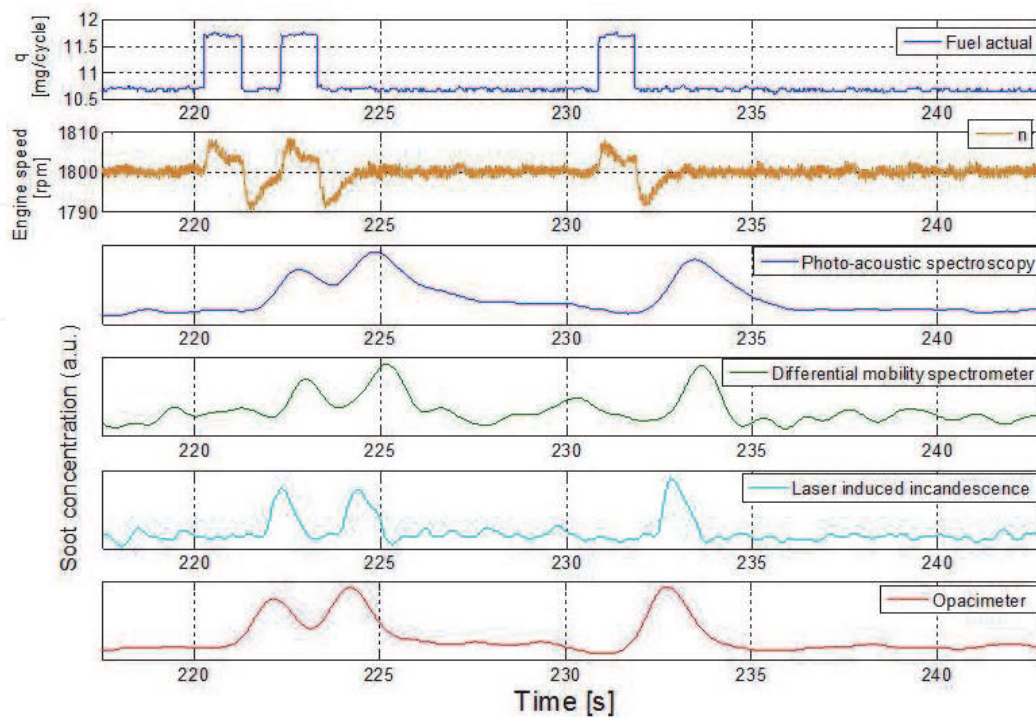


Figure 9. The injected fuel, engine speed and filtered data of soot concentration measured by photoacoustic spectroscopy, differential mobility spectrometer, opacimeter and laser-induced incandescence within 1000 ms pulses injected at 10.7 mg/cycle fuel load are shown.

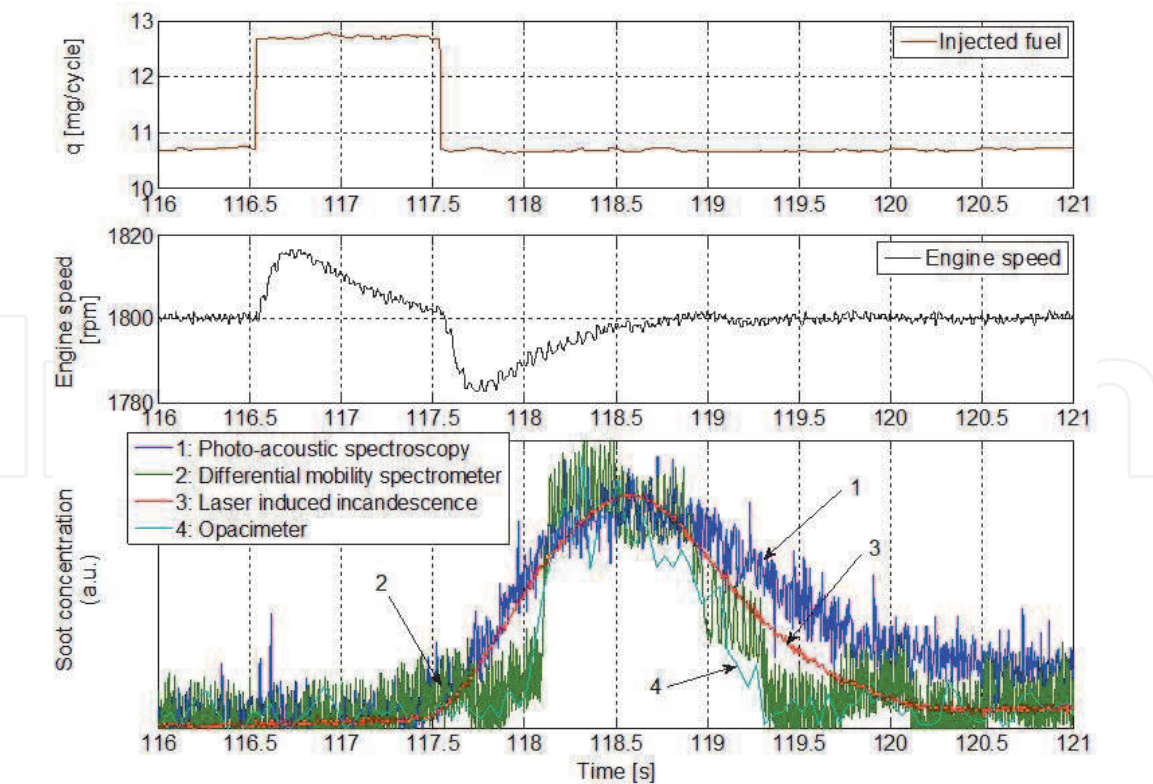


Figure 10.
Single 1000 ms pulse of injected fuel shows engine speed and raw data of soot concentration measured by photoacoustic spectroscopy, differential mobility spectrometer, opacimeter and laser-induced incandescence at constant 10.7 mg/cycle fuel load.

this measurement the differences in measured speed to fast transient peak and dynamic response of devices are well differentiated.

In **Figure 11** filtered data from selected upslope (rise time) of soot emission from a single peak, normalised to 100%, are shown. Measured peak response from devices was shifted so that the maximum 100% of soot concentration is located in zero-time coordinate. The largest negative time value, where the function has x-intercept (zero concentration), corresponds to the slowest measured response, in

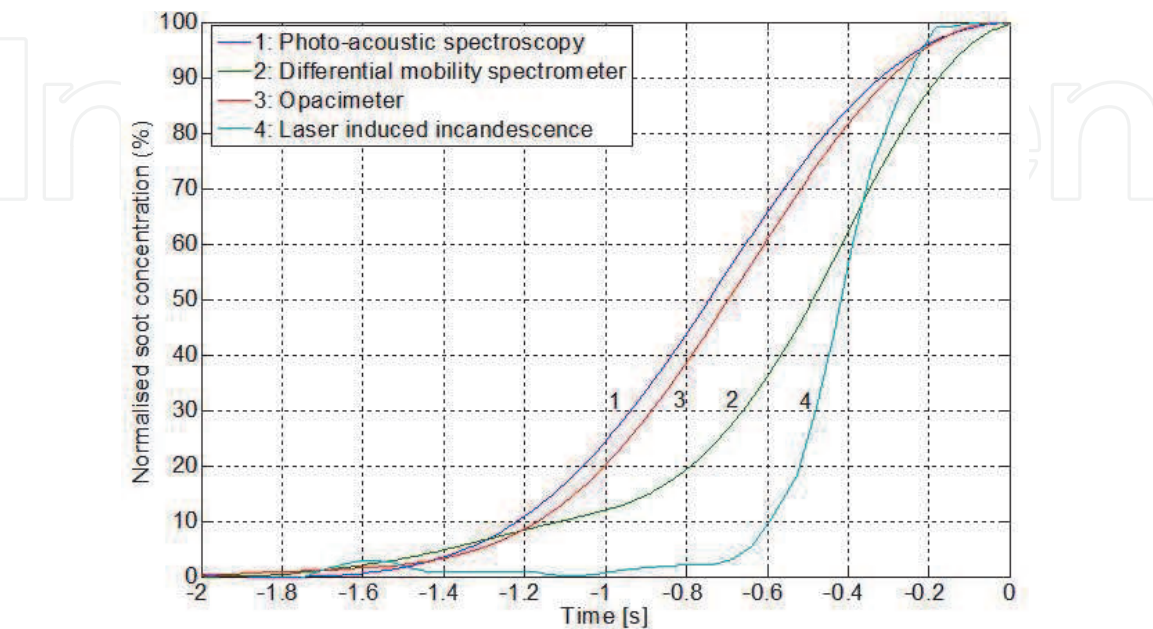


Figure 11.
Filtered data of normalised upslope (rise time) peak from selected part of test soot emission. Note the negative time delay.

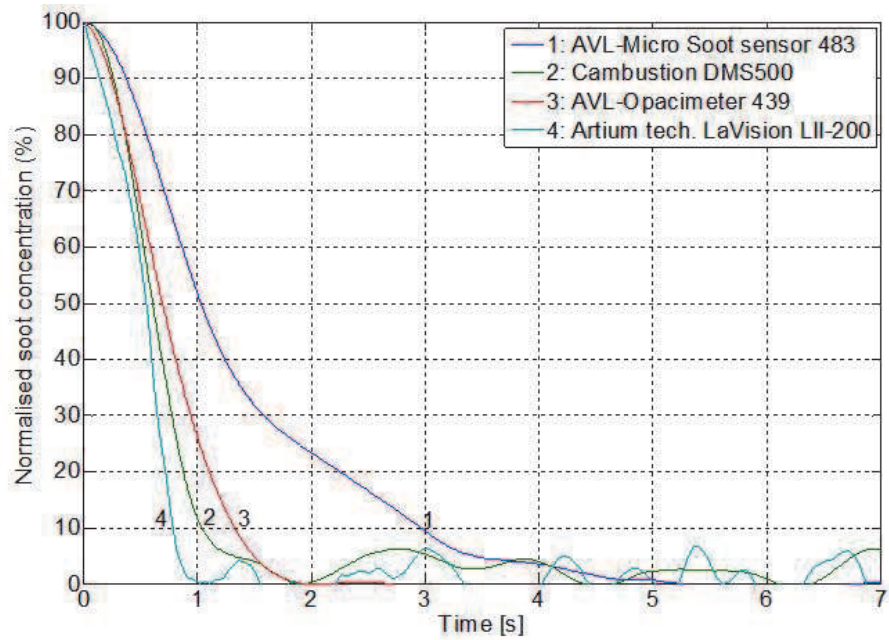


Figure 12.
Filtered data of normalised downslope (fall time) peak from selected part of test soot emission.

this case to photoacoustic spectroscopy (1). The steepest slope and the fastest rise time of soot level have been measured by the laser-induced incandescence (4).

In **Figure 12** the filtered data from selected downslope (fall time) peak of soot emission normalised to 100% are shown. Resulting data shows similar tendency. The steepest decay was measured by the laser-induced incandescence, the second fastest by the differential mobility spectrometer and opacimeter. The slowest response was measured by photoacoustic spectroscopy device.

Measured rise time during upslope peak, normalised soot concentration from 10 to 90% and downslope (fall time) peak from 90 to 10% are summarised in **Table 2**.

Obtained results are better pronounced in a bar graph (**Figure 13**). Here, an overview of measured rise time (10–90%) and fall time (90–10%) of normalised soot concentration emission measured from 1000 ms injection peak during static pulse test at 10.7 mg/cycle fuel load are shown.

4.4 Dynamic transient measurements

Comparison of the results from dynamic transient test PM emission measurement during standard New European Driving Cycle measured by photoacoustic

	Up-slope time (s) 10% –90%	Down-slope time (s) 90%–10%
Photo-acoustic spectroscopy	0.89	2.59
Differential mobility spectrometer	0.93	0.77
Opacimeter	0.86	1.08
Laser Induced Incandescence	0.34	0.64

Table 2.
Summary of measured upslope (rise) time from 10 to 90% and downslope (fall) time from 90 to 10% of normalised soot concentration measured from 1000 ms injection peak during static pulse test at 10.7 mg/cycle fuel load.

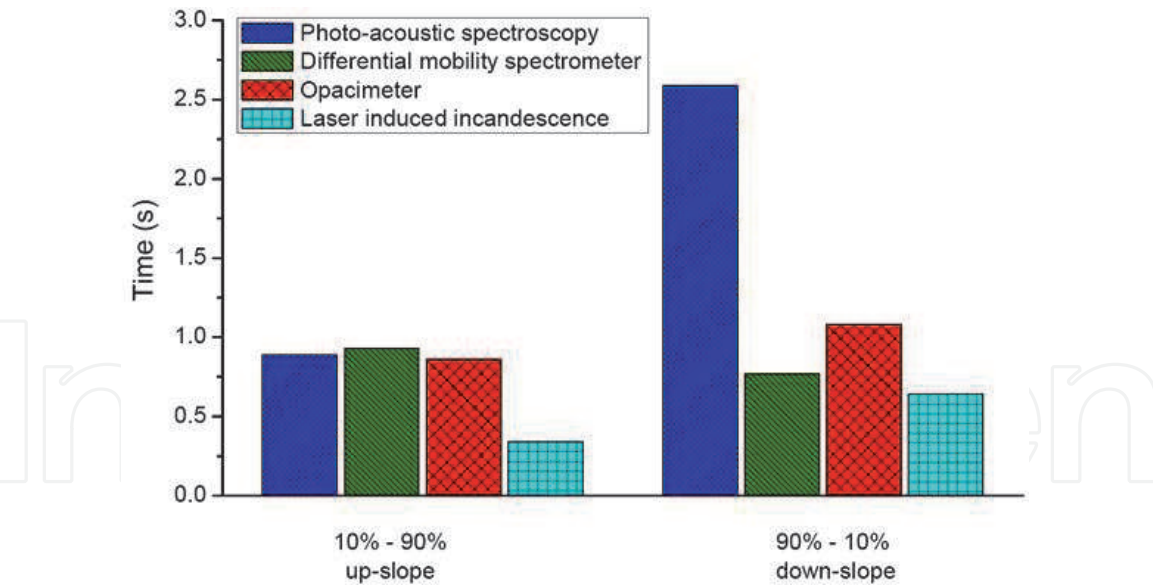


Figure 13.
The overview of measured rising (10–90%) and falling (90–10%) time of normalised soot emission concentration measured from 1000 ms injection peak during static pulse test at 10.7 mg/cycle fuel load.

spectroscopy, differential mobility spectrometer, opacimeter and laser-induced incandescence method is shown in **Figure 14**. Shown recorded data are in raw, not filtered format. The time delay has been individually shifted, in such a way that the signals were overlapped in the centre of the first transient measured peak. Generated time delay of the individual devices is caused by the different length of the sampling line to the detectors. It has to be considered that recording of the signal via dSpace board is not continuous, but it has a saving procedure in approximately

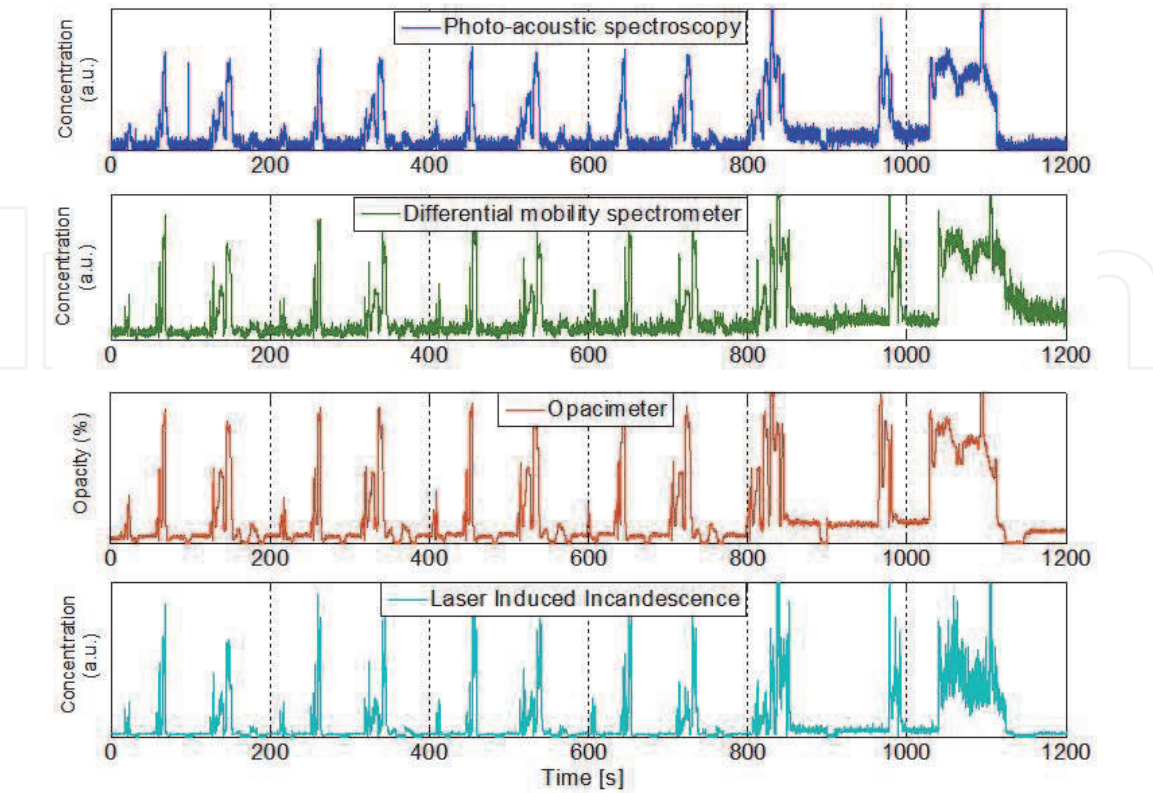


Figure 14.
Raw data shows comparison of transient test soot emission during NEDC cycle measured by photoacoustic spectroscopy, differential mobility spectrometer, opacimeter and laser-induced incandescence.

every 400 seconds. Hence, the signals experience recorded gaps in a duration of approximately 4 seconds. This generates a shift in NEDC data, mainly visible at the end of the cycle in the case of photoacoustic and opacimeter devices.

Generally, all instruments have shown similar response to soot emission, without cut-off in signal during measurement. Main differences are noticeable in the soot emission measured mainly during the fast transient peaks. In the case of differential mobility spectrometer, the continuously increasing background level of soot emission, mainly visible in the second part of the NEDC cycle, is conspicuously observed. However, this can negatively affect the precision of measurement. This effect can be associated with the increasing gas emission temperature during the NEDC cycle itself and due to the downstream of the turbine sensor location in the exhaust manifold. In **Figure 15** the injected fuel to the engine as an input parameter and output parameters measured pressure and temperature from the location downstream of the turbine are shown. The temperature of gas emission is continuously increasing from 90°C at the beginning of the test cycle up to 205°C nearly at the end of the NEDC test cycle at this measurement location.

Commonly, all devices are taking partial stream emission measurement through heated sample line to the measuring cells. In this cell, the temperature of the measured gas is stabilised and compensated. However, the incoming gas temperature is limited to the maximum recommended value during the measurement, shown in **Table 1**, where the upper temperature limit for DMS is specified to 150°C. Therefore, a measurement above these temperature limits should be taken with the higher uncertainty for the DMS device. Besides the temperature in the manifold, a very important parameter is the gas pressure signal. In **Figure 15** one can observe fast dynamic changes in pressure of exhaust emissions, inside the exhaust manifold, particularly downstream of the turbine position, due to fast dynamic NEDC test cycle measurement. The pressure here varies from 960 to 1800 mbar. For that reason, measurement devices usually dilute the exhausted gas before it is essentially

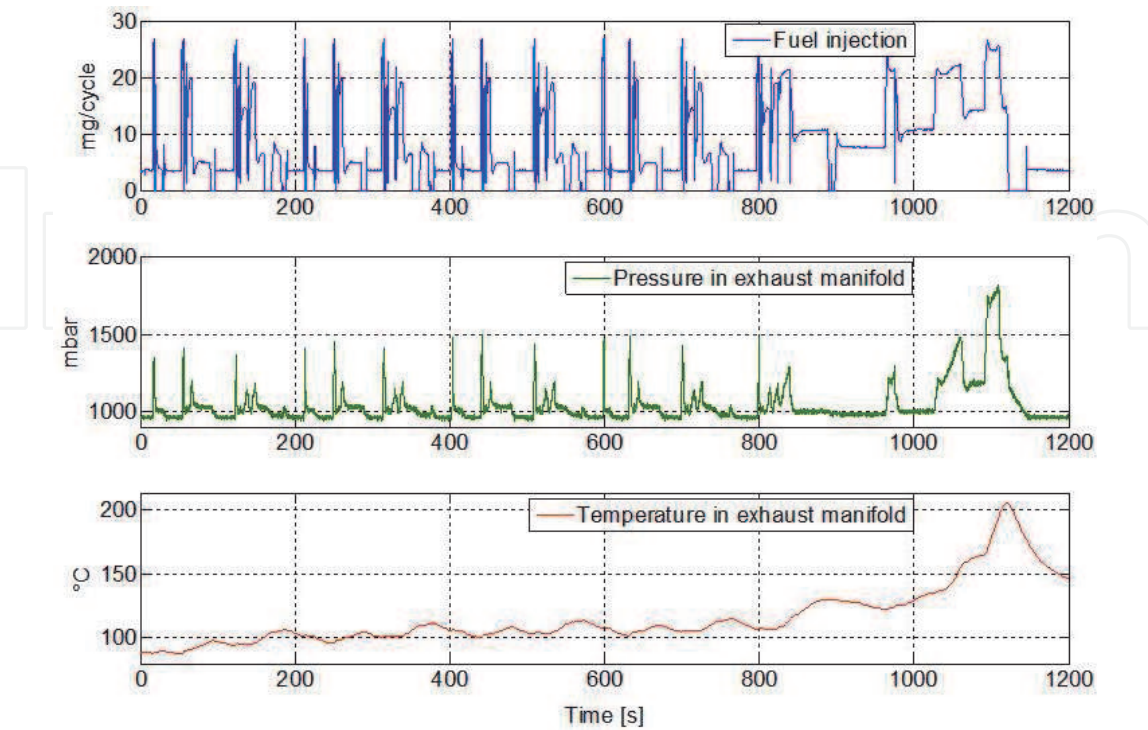


Figure 15. Graph shows injected fuel into the engine as an input parameter and output parameters measured pressure and temperature from the location downstream of the turbine in the exhaust manifold during one NEDC cycle.

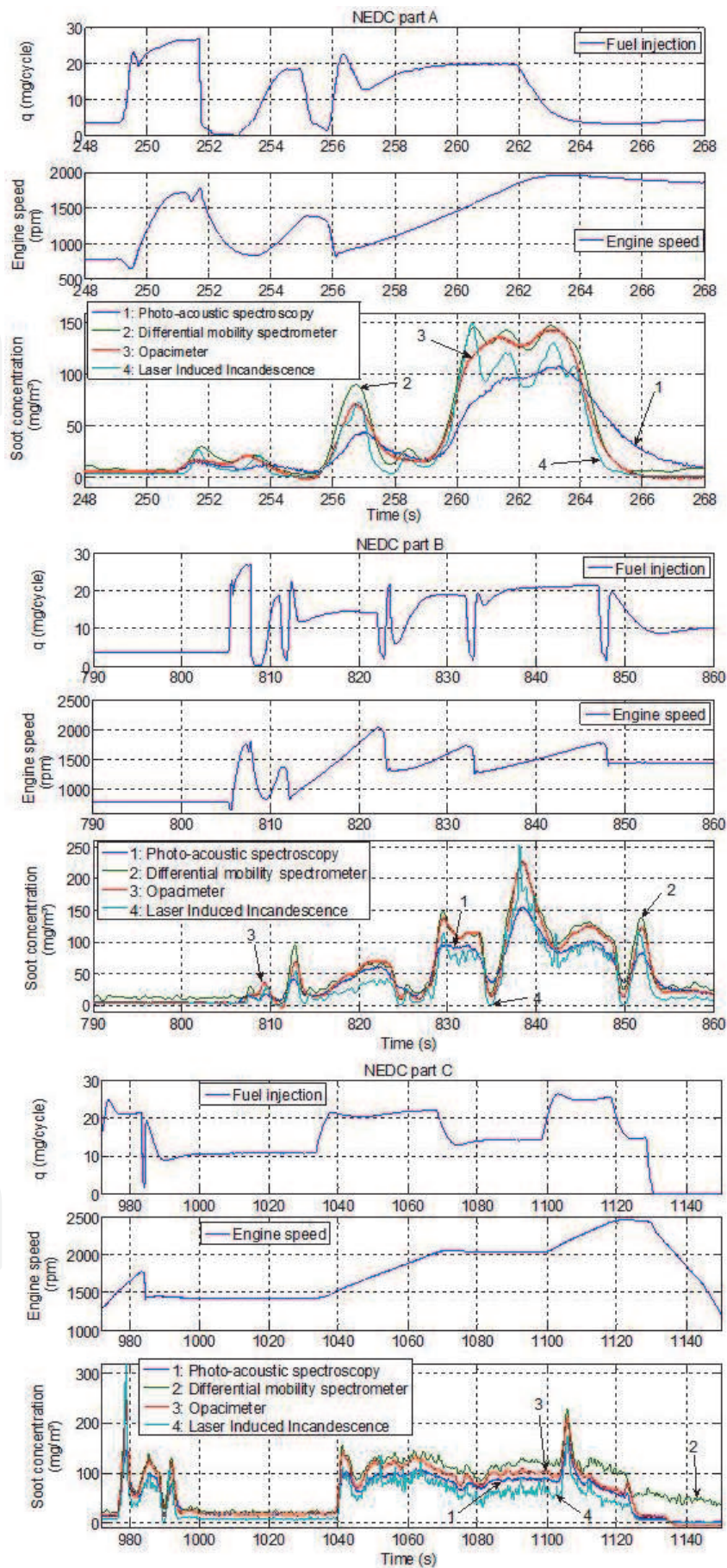


Figure 16. Selected three parts A, B, and C of the NEDC test cycle show the input parameters of fuel injection function (mg/cycle) and the engine speed (rpm). Soot emissions were simultaneously measured by photoacoustic spectroscopy (1), differential mobility spectrometer (2), opacimeter (3) and laser-induced incandescence (4) devices.

measured. To maintain a constant volume sampling (CVS), total flow of exhaust gas emission is kept constant during the measurement in dilution tunnel. On the other hand, diluting an exhaust gas can negatively influence the measurement with low concentration of soot emission, because soot particles might not be detected.

In **Figure 16** three selected parts of the NEDC test cycle are shown in detail: first part A from 248 to 268 seconds, second part B from 790 to 860 seconds and third part C from 970 to 1150 seconds. Additional input parameters are fuel injection function (mg/cycle) and the engine speed profile in rotation per minute (rpm). In these figures differences between transient emission peaks in measured profile by four devices are significantly pronounced.

On bases of measured soot concentrations from NEDC, one can easily differentiate from the point of sensitivity measurement devices into two groups. First is the group with higher temporal resolution of the measured soot emission signal, with more like spiky profiles. In the first group, the signals from laser-induced incandescence and differential mobility spectrometer can be considered. The second group has a lower temporal resolution and more smooth concentration function profile. In this group the signal measured via photoacoustic spectroscopy and opacimeter can be included. An advantage of devices in the first group is that these are capable to resolve sensitive emission fluctuation and fast transient peaks in soot dynamic signal, better than the second and slower group.

5. Conclusions

In this book chapter, the comparison between the five different commercially available techniques for soot and particulate matter emission measurement from diesel engine is shown. The comparison has been made from static and dynamic transient measurement tests with special concern to compare the sensitivity and dynamics response of individual methods. Measurements were performed by filter-type smoke meter, from AVL Smoke meter 415S; by photoacoustic spectroscopy, from AVL Micro soot sensor 483; by differential mobility spectrometer from Cambustion model DMS 500 and opacimeter from AVL Opacimeter 439; and by laser-induced incandescence from Artium Technologies Inc. LII 200. The filter-type smoke meter was selected due to conventional use as a standard device for measurement of soot concentration. The other fast devices were selected due to their relatively high accuracy and fast response, which is often needed for characterisation of soot and PM during the combustion process. Devices were placed in to the location downstream of the turbine, to be as close to the actual combustion event. All instruments have shown similar response to soot emission with no cut-off or disruption in measured signal. However, detailed time-resolved measurements during static and dynamic transient tests revealed differences in sensitivity and dynamics response of individual methods. From the point of view of sensitivity, the laser-induced incandescence and differential mobility spectrometer resolved small oscillations in soot emissions during fast transient's measurement with higher temporal resolution than the opacimeter or photoacoustic spectrometer. The dynamics response was measured from the slope of static peaks with individual concern to upslope and downslope of normalised soot concentration. In any case, the fastest technique has been laser-induced incandescence, then the differential mobility spectrometer, afterwards the opacimeter and in the last place the signal from the photoacoustic spectrometer. Compared measurements provide useful information concerning sensitivity and dynamics characteristics of the selected techniques for static and dynamic measurements of soot and particulate matter emissions from diesel engine.

Acknowledgements


The author would like to thank Mr. Richard Fürhapter and Mr. Gerhard Wurzinger for their perfect test bench support, and to Austrian Research Promotion Agency (FFG) and to Austrian Science Fund, FWF (Fonds zur Förderung der wissenschaftlichen Forschung) for providing financial support. Part of this study was funded with the grant number FWF—P27967. This work has been also supported by the COMET-K2 Center of the Linz Center of Mechatronics (LCM), funded by the Austrian federal government and the federal state of Upper Austria. Additionally, the author would like to thank Dr. Maria Rusnak for the proofreading and for valuable corrections.

Author details

Richard Viskup
Johannes Kepler University Linz, Linz, Austria

*Address all correspondence to: richard.viskup@jku.at; viskup@gmail.com

IntechOpen

© 2020 The Author(s). Licensee IntechOpen. This chapter is distributed under the terms of the Creative Commons Attribution License (<http://creativecommons.org/licenses/by/3.0>), which permits unrestricted use, distribution, and reproduction in any medium, provided the original work is properly cited. 

References

- [1] Lighty JS, Veranth JM, Sarofim AF. Combustion aerosols: Factors governing their size and composition and implications to human health. *Journal of the Air and Waste Management Association*. 2000;**50**(9):1565-1618. DOI: 10.1080/10473289.2000.10464197
- [2] McAdam K, Steer P, Perrotta K. Using continuous sampling to examine the distribution of traffic related air pollution in proximity to a major road. *Atmospheric Environment*. 2011;**45**(12):2080-2086. DOI: 10.1016/j.atmosenv.2011.01.050
- [3] Wichmann HE, Peters A. Epidemiological evidence of the effects of ultrafine particle exposure. *Philosophical Transactions of the Royal Society of London, Series A: Mathematical, Physical and Engineering Sciences*. 2000;**358**(1775):2751-2768. DOI: 10.1098/rsta.2000.0682
- [4] Burtscher H. Physical characterization of particulate emissions from diesel engines: A review. *Journal of Aerosol Science*. 2005;**36**(7):896-932. DOI: 10.1016/j.jaerosci.2004.12.001
- [5] ACEA program on emissions of fine particles from passenger cars. Available from: www.acea.be
- [6] Vouitsis E, Ntziachristos L, Samaras Z. Particulate matter mass measurements for low emitting diesel powered vehicles: What's next? *Progress in Energy and Combustion Science*. 2003;**29**(6):635-672. DOI: 10.1016/j.pecs.2003.08.002
- [7] Ayrault C, Chang JS, Ewing D, Cotton JS, Gerges IE, Burgers J. Differential thermal analysis, thermal gravimetric analysis, and solid phase micro-extraction gas chromatography analysis of water and fuel absorption in diesel soot. *Journal of Aerosol Science*. 2010;**41**(2):237-241. DOI: 10.1016/j.jaerosci.2009.10.006
- [8] Choi MY, Mulholland GW, Hamins A, Kashiwagi T. Comparisons of the soot volume fraction using gravimetric and light extinction techniques. *Combustion and Flame*. 1995;**102**(1-2):161-169. DOI: 10.1016/0010-2180(94)00282-W
- [9] Main RP, Bauer E. Opacities of carbon-air mixtures at temperatures from 3000-10000 degrees K. *Journal of Quantitative Spectroscopy & Radiative Transfer*. 1966;**6**(1):1-30. DOI: 10.1016/0022-4073(66)90061-6
- [10] Zahoransky RA, Saier T, Laile E, Nikitidis M, Konstandopoulos A. Optical Multiwavelength Technique Applied to the Online Measurement of Particle Emissions from Engines. SAE Paper No. 2001-01-047. 2001. DOI: 10.4271/2001-24-0074
- [11] Schneider J, Weimer S, Drewnick F, Borrmann S, Helas G, Gwaze P, et al. Mass spectrometric analysis and aerodynamic properties of various types of combustion-related aerosol particles. *International Journal of Mass Spectrometry*. 2006;**258**(1-3):37-49. DOI: 10.1016/j.ijms.2006.07.008
- [12] Symonds JPR, Reavell KSJ, Olfert JS, Campbell BW, Swift SJ. Diesel soot mass calculation in real-time with a differential mobility spectrometer. *Journal of Aerosol Science*. 2007;**38**(1):52-68. DOI: 10.1016/j.jaerosci.2006.10.001
- [13] Filipi Z, Hagena J, Fathy H. Investigating the impact of in-vehicle transients on diesel soot emissions. *Thermal Science*. 2008;**12**(1):53-72. DOI: 10.2298/TSCI0801053F
- [14] Faxvog FR, Roessler DM. Optoacoustic measurements of diesel particulate-emissions. *Journal of Applied Physics*. 1979;**50**(12):7880-7882. DOI: 10.1063/1.325978

- [15] Adams KM. Real-time insitu measurements of atmospheric optical absorption in the visible via photoacoustic-spectroscopy 1. Evaluation of photoacoustic cells. *Applied Optics*. 1988;27(19):4052-4056. DOI: 10.1364/AO.27.004052
- [16] Beck HA, Niessner R, Haisch C. Development and characterization of a mobile photoacoustic sensor for on-line soot emission monitoring in diesel exhaust gas. *Analytical and Bioanalytical Chemistry*. 2003;375(8):1136-1143. DOI: 10.1007/s00216-003-1810-8
- [17] Snelling DR, Smallwood GJ, Sawchuk RA, Neill WS, Gareau D, Clavel D, et al. Particulate Matter Measurements in a Diesel Engine Exhaust by Laser-Induced Incandescence and the Standard Gravimetric Procedure. SAE Paper No. 1999-01-3653. 1999. DOI: 10.4271/1999-01-3653
- [18] Axelsson B, Witze PO. Qualitative Laser-Induced Incandescence Measurements of Particulate Emissions During Transient Operation of a TDI Diesel Engine. SAE Paper No. 2001-01-3574. 2001. DOI:10.4271/2001-01-3574
- [19] Witze PO, Payne GA, Bachalo WD, Smallwood GJ. Influence of Measurement Location on Transient Laser-Induced Incandescence Measurements of Particulate Matter in Raw Diesel Exhaust. SAE Paper No. 04ANNUAL-174. 2004
- [20] Thomson KA, Snelling DR, Smallwood GJ, Liu F. Laser induced incandescence measurements of soot volume fraction and effective particle size in a laminar co-annular non-premixed methane/air flame at pressures between 0.5-4.0 MPa. *Applied Physics B: Lasers and Optics*. 2006; 83(3):469-475. DOI: 10.1007/s00340-006-2198-x
- [21] Viskup R, Alberer D, Oppenauer K, del Re L. Measurement of Transient PM Emissions in Diesel Engine. SAE Technical Paper 2011-24-0197. 2011. DOI:10.4271/2011-24-0197
- [22] Viskup R, Alberer D, Oppenauer K, del Re L. Fast detection of transient emission from diesel engine using optical and differential mobility spectrometer method. *Technisches Messen*. 2011;78(11):520-525. DOI: 10.1524/teme.2011.0207
- [23] Oppenauer K, Alberer D, del Re L. Control Oriented Crank Angle Based Analysis of Soot Dynamics During Diesel Combustion, SAE Powertrains. SAE Paper No. 2010-01-2105. 2010. DOI:10.4271/2010-01-2105
- [24] Alberer D, del Re L. Optimization of the Transient Diesel Engine Operation. SAE Paper No. 2009-01-0622. 2009. DOI:10.4271/2009-24-0113
- [25] Alberer D, del Re L, Winkler S, Langthaler P. Virtual Sensor Design of Particulate and Nitric Oxide Emissions in a DI Diesel Engine. SAE Paper No. 2005-24-063. 2005. DOI:10.4271/2005-24-063
- [26] Dasch CJ. Continuous-wave probe laser investigation of laser vaporization of small soot particles in a flame. *Applied Optics*. 1984;23(13):2209-2215. DOI: 10.1364/AO.23.002209
- [27] Alberer D. Fast oxygen based transient diesel engine control [Dissertation]. Linz, Austria: Johannes Kepler University, JKU; 2009
- [28] Smoke value measurement with the filter paper method [Application Notes]. AT1007E, Rev. 02, AVL List. Graz, Austria: GmbH; 2005